Available online at www.sciencedirect.com
SCIENCE DIRECT®
Journal of Nuclear Materials 351 (2006) 78–87
journal of nuclear materials
www.elsevier.com/locate/jnucmat

Kinetic Monte Carlo simulations applied to irradiated materials: The effect of cascade damage in defect nucleation and growth

M.J. Caturla [a,*], N. Soneda [b], T. Diaz de la Rubia [c], M. Fluss [c]

[a] Departamento de Fisica Aplicada, Universidad de Alicante, Alicante E-03690, Spain
[b] CRIEPI, Central Research Institute of Electric Power Industry, 2-11-1 Iwado-kita, Komae-shi, Toko 201, Japan
[c] Chemistry and Materials Science Dir., Lawrence Livermore National Laboratory, Livermore, CA 94550, USA

Abstract

Kinetic Monte Carlo is used extensively in the field of radiation effects to understand damage accumulation and growth under irradiation. These calculations require previous knowledge on the formation of these defects, the relative stabilities of the different types of defects, their interactions and their mobilities. Many of these parameters can be extracted from molecular dynamics calculations using empirical potentials or from ab initio calculations. However, the number of parameters necessary for a complete picture is rather large. Kinetic Monte Carlo can be used as a tool to isolate those parameters that most influence the outcome of the calculations. In this paper, we focus on one aspect: the form of the damage after the collision cascade. We describe the effect of the form of the cascade as obtained from molecular dynamics simulations on damage accumulation. In particular, we demonstrate that the form of the cascade drastically changes the nucleation and growth of helium-vacancy clusters, possible precursors of voids and bubbles. Finally, we point to those open questions that need to be resolved to develop a truly predictive kinetic Monte Carlo model.

PACS: 61.82.Bg; 61.80.Az; 66.30.Lw

1. Introduction

Kinetic Monte Carlo (kMC) calculations are nowadays commonly used to model the evolution of damage in irradiated materials in order to extend the time scale of molecular dynamics (MD) simulations to those times achieved in experiments. This method was first described by Besco in the late 1960s [1] and used by Doran and Burnett [2,3] for short-term annealing of cascades. The extensive use of kMC, however, did not start until the early 1990s with the work of Heinisch [4] using input data from MD simulations. Currently several research groups perform kMC calculations of radiation effects in materials [5–9]. This method is also used in the field of ion implantation of semiconductors to model dopant diffusion and clustering [10,11].

This powerful tool requires previous knowledge of the type of defects produced during irradiation,

* Corresponding author. Tel.: +34 965 90 3400x2056; fax: +34 965 90 9726.
E-mail address: mj.caturla@ua.es (M.J. Caturla).

0022-3115/$ - see front matter © 2006 Elsevier B.V. All rights reserved.
doi:10.1016/j.jnucmat.2006.02.019

the mobilities of such defects, their stability and the interaction between defects and with the microstructure. Tools such as molecular dynamics and ab initio calculations have been very useful in understanding damage production in different metals. In particular, molecular dynamics simulations have shown in the last two decades that the damage produced by energetic atoms can be very different in f.c.c. and b.c.c. structures [12–15]. In f.c.c. metals the damage produced after the cascade collapse consist of clustered vacancies and self-interstitials [12–14] formed within a few picoseconds. This behavior has been observed in Cu [12–14], Au [16] and Pb [17] and at a lower extent in Ni [18]. On the other hand, damage in b.c.c. metals such as Fe consists mostly of isolated or small vacancy clusters and small self-interstitial clusters [15]. The same type of behavior has been observed also in W [19]. The reason for these differences in clustering is not completely understood. Some studies point towards a difference in recrystallization rates during cascade cooling as an important factor in clustering [18]. Others argue that the high stacking fault energies of b.c.c. metals could be the reason for these differences.

The stability and mobility of defects has also been studied using molecular dynamics simulations. Self-interstitial clusters are very stable with high binding energies and they diffuse very rapidly one-dimensionally according to exhaustive MD simulations [20–22]. Recent ab initio calculations [23,24] have shown that in the case of Fe the lowest energy configuration is a $\langle 1\,1\,0\rangle$ dumbbell instead of the $\langle 1\,1\,1\rangle$ dumbbell predicted by earlier calculations using embedded atom type of interatomic potentials [21,22,25]. This implies a higher migration energy for the single interstitial and small clusters in Fe as well as a three-dimensional diffusion. For clusters with four or more interstitials the $\langle 1\,1\,1\rangle$ configuration is probably still the most stable, and one-dimensional migration with low migration energies are also expected.

Our knowledge on the interaction between defects and impurities is still limited. Probably the one impurity that has been studied the most using MD is helium. It is known that metals exposed to radiation can alter significantly their volume particularly in the presence of gases such as He or H [26]. This phenomenon is known as void swelling and has been given special attention in the field of radiation effects in structural materials for fission and fusion reactors [27]. Despite many years of research in this topic there are still many unknowns regarding the initial stages of nucleation of those defects responsible for the dimensional changes in these metals.

The processes involved in radiation induced volume changes are multiple and intricate. In general, it results from differences in the distribution of those vacancies and self-interstitials produced during irradiation. The damage produced by an energetic atom consists of an equal number of vacancies and self-interstitials. Self-interstitials diffuse to sinks such as grain boundaries, dislocations or surfaces, leaving in the bulk an excess of vacancies. These vacancies, at high enough temperatures, can diffuse and form larger clusters. The presence of an element such as He can stabilize the vacancy clusters into a three-dimensional defect configuration (voids or bubbles) impeding the collapse of these structures into loops and resulting in a net gain in volume of the system. The different behavior between vacancies and self-interstitials was first explained by a preferential trapping of interstitials to dislocations, due to their stronger elastic interaction with the dislocation stress field. This model was called dislocation bias [28] and was very successful in explaining swelling rates of different metals at high doses. Differences in void swelling observed between f.c.c. and b.c.c. materials were explained by this model through a difference in the dislocation bias for these two structures. There were, however, experiments that could not be explained by this model, such as the swelling rates of pure metals at low doses and dislocation densities [29]. In order to explain these experimental results a new model was proposed based on results from MD simulations called the 'production bias' model [30]. Models used to study cavities in metals under irradiation are based on continuum equations.

With the information provided by the MD calculations it has been possible to perform kMC simulations in pure metals, such as Cu or Fe, [4–9] or in metals in the presence of He to study the first stages of He–V cluster formation [31]. However, there are still many unknowns, in particular regarding the interaction between defects and impurities. The number of variables needed to fully describe all the processes occurring is so large that it would not be possible to obtain them directly from MD calculations. Therefore, it is important to have an understanding of those parameters in the calculation that significantly affect the results. In this paper we will focus on the influence of the distribution of vacancies and self-interstitials from the collision cascade just after a few picoseconds as obtained from

MD simulations, on damage accumulation and growth. First we will review some earlier work on Cu and Fe that already pointed to the significance of this parameter. Then we will describe the effect in the nucleation and growth of He–V clusters, possible precursors for bubbles and voids.

In the next section we describe the particular kMC approach used in the calculations. In Section 3 we review some of the studies of damage accumulation in Cu and Fe using kMC simulations. In Section 4 we describe calculations of defect accumulation in the presence of helium. These calculations show the importance of the cascade damage and reveal some interesting features associated with the nucleation and growth of He–V clusters. The consequences of these calculations are explained in Section 5 together with some discussion about the steps that need to be taken in order to develop a predictive and efficient kMC model for damage accumulation.

2. Kinetic Monte Carlo applied to radiation damage

The name kinetic Monte Carlo is often used to describe different types of algorithms that involve an evolution in time. Therefore, we would like to first describe in detail the particular algorithm used for those calculations reported below. A name currently used to describe this algorithm is Object Kinetic Monte Carlo (OKMC). It follows the evolution of a set of objects in time, given the type of events those objects can perform and the probability for each event to occur. In the case of radiation the objects of interest are those defects produced during the irradiation, that is vacancies, self-interstitials, impurities and their clusters. The events these objects can perform are diffusion events, dissolution from a cluster, interaction between different defects or defects with other objects such as grain boundaries or dislocations. The probabilities of these events are given by the migration energies and binding energies of the defects. For example, the probability of a defect of type i undergoing a migration event is given by

$$\Gamma^i_{\mathrm{m}} = \Gamma^i_0 \exp(-E^i_{\mathrm{m}}/KT), \tag{1}$$

where Γ^i_0 is the jump frequency, E^i_{m} is the migration energy for that particular defect, K is Boltzmann's constant and T is the temperature. When a migration event is selected the object is moved a distance δ the jump distance, which is often selected between first and second nearest neighbors. When the object can migrate in any direction (three-dimensional migration) the jump is performed by randomly placing the object within a sphere of radius δ. When the migration of the object is restricted to one particular direction (one-dimensional migration), such as the case of self-interstitial clusters mentioned above, a particular direction of motion ($\langle 1\,1\,1\rangle$ for Fe and $\langle 1\,1\,0\rangle$ for Cu, for example) with respect to the simulation box is given to the object when it is created, and the jumps are performed only along that direction and with a distance δ.

The probability of a defect of type i undergoing a dissolution event from a cluster is given by

$$\Gamma^i_{\mathrm{d}} = \Gamma^i_0 \exp(-(E^i_{\mathrm{m}} + E^i_{\mathrm{b}})/KT), \tag{2}$$

where E^i_{b} is the binding energy of the defect to the cluster. This energy depends on the number of defects in the cluster.

The kMC algorithm proceeds by selecting an event from all the possible ones. First, the total rate for all events is calculated as

$$R = \sum_{\mathrm{e}} \Gamma_{\mathrm{e}} N_{\mathrm{e}}, \tag{3}$$

that is the sum over all events of the probability of each event Γ_{e}, as calculated by Eqs. (1) or (2) above, times the number of objects that can undergo that event, N_{e}. An event is chosen randomly between 0 and R, therefore ensuring that each event is weighted by the appropriate probability of occurrence. The time of the simulation is then increased by Δt

$$\Delta t = \frac{-\log \xi}{R}, \tag{4}$$

where R is the total rate give by Eq. (3) and ξ is a random number between 0 and 1, that is used to give a Poisson distribution of the time. Once the event has been selected a random particle is chosen from all those that can undergo that event.

The initial conditions of the simulation are the (x, y, z) coordinates of those defects produced by the irradiation as well as their type. In case of a continuous irradiation, new defects are introduced in the simulation box with a rate according to the dose rate of the experiment that is being simulated. The positions and types of defects are obtained from molecular dynamics, from binary collision approximation (BCA) calculations, such as those obtained from SRIM [32] or Marlow [33], or as a random distribution of Frenkel-pairs, depending on the type

of calculation. For example, when damage is produced by electrons the last approximation can be used [34]. In the case of damage produced by light ions such as He, calculations using the binary collision approximation are appropriate. However, for self-irradiation and heavy-ions it is necessary to use those results obtained from MD simulations. Oftentimes a combination of BCA and MD calculations is used to obtain the distribution of defects during irradiation for energies that cannot be reached by MD alone. In this case the BCA is used to obtain the energies of those recoils produced by the energetic particle along its path, but the final defect distribution produced by those recoils is the one obtained from MD simulations. This approximation is based on the existence of a threshold for sub-cascade formation.

Most of the kMC calculations for radiation effects in metals describe the objects as points in the simulation box with a capture radius that depends on the number of defects of that object. This capture radius is normally defined spherical as

$$r_n = \sqrt[3]{\frac{3n\Omega}{4\pi}}, \tag{5}$$

where n is the number of defects in the cluster and Ω is the atomic volume. This capture radius is used to define when two defects interact. Also when a defect dissolves from a cluster it is positioned outside this capture radius. When using this approach information regarding the lattice structure is lost. It is however possible to keep the location of every defect during the calculation with the consequent increase in memory for the calculation. This is in fact done in models of dopant diffusion in silicon [11]. Strain effects such as the bias interaction between interstitials and dislocations can be included in this capture radius, increasing the capture radius for interstitials. However, it is also possible to include strain effects in kMC using elasticity theory [35,36].

3. Damage accumulation in Cu and Fe

KMC simulations have been used to study the damage accumulation in Cu and Fe under irradiation [4–9]. These calculations have helped to understand the differences observed in transmission electron microscopy (TEM) measurements of defect densities in these materials [37]. The defect densities measured by TEM in Fe are at least one order of magnitude lower than for the case of Cu. Moreover, over 90% of those defects observed in Cu are stacking fault tetrahedral (SFT) [29], and the average size of these defects does not change with irradiation dose, remaining between 2 and 3 nm in size. In Fe, however, those defects observed in the microscope are interstitial type [38]. As an example we show in Fig. 1 the concentration of visible defects as a function of dose for Cu and Fe as obtained from kMC simulations [8]. In these calculations visible clusters are for the case of vacancy clusters those with more that 20 vacancies, which corresponds to a SFT of approximately 1.5 nm side, and for the case of interstitial clusters those with more than 50 defects, corresponding to loops of about 1 nm radius.

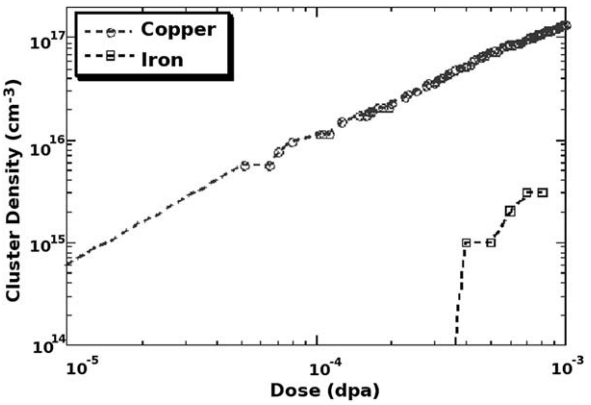

Fig. 1. Concentration of visible defects as a function of dose in Cu (circles) and Fe (squares) as obtained from kMC simulations. Figure from Ref. [8].

The kMC calculations provide an explanation for the origin of these differences. There are two features responsible for these results. The most significant is the difference in the damage after the cascade collapse. As mentioned above MD simulations have shown that in the case of Cu most of the vacancies are clustered while in the case of Fe most of them are isolated. As a result, those defects produced directly in the cascade are large enough to be resolved in the TEM. This also explains the constant average size with dose observed in these experiments, as well as the simulations. In the case of Fe vacancy clusters are very small and cannot be resolved with TEM. However, positron annihilation experiments have shown the presence of small vacancy clusters in Fe [39]. These small vacancy clusters also appear in kMC calculations, with sizes of around 4–5 vacancies per cluster on average and their concentration has also been reproduced by KMC models [6,9].

The second significant difference is the effect of impurities in the evolution of damage, in particular,

in the mobility of self-interstitial clusters. MD simulations predict that self-interstitial clusters have very low migration energies for all sizes studied [20–22]. In order to reproduce the experimental observation of self-interstitial clusters in Fe an effective trapping mechanism must be included in the KMC simulations for these clusters [6,7,9]. Different approaches are used for this effective trapping. In some cases self-interstitial clusters larger than some size are considered sessile [9], in other cases a binding between impurities and self-interstitial is included in the calculation [6]. This trapping mechanism is in fact one of the key parameters in these calculations that needs more study (see Ref. [6] for further discussion). Details regarding the mechanism of trapping of self-interstitials by impurities is not yet clear. Ab initio calculations indicate weak interaction between SIA and impurities such as C and N [40]. Other possible trapping mechanisms have also been considered due to elastic interactions between impurities and self-interstitials [35]. Further ab initio calculations as well as KMC calculations including elastic interactions will have to be performed to have a better description of this effect. Finally, another experimental observation that needs to be resolved for the case of Fe is the presence of both $\langle 1\,1\,1\rangle$ and $\langle 1\,0\,0\rangle$ loops. MD simulations point to some possible mechanisms for the formation of these $\langle 1\,0\,0\rangle$ loops [41].

4. Helium-vacancy cluster nucleation and growth

In order to elucidate the role of the initial damage structure produced during the collision cascade in the nucleation and growth of He–V clusters we have developed a kMC model with input parameters obtained from MD. The interactions described in our model include interstitial, vacancy and He migration and clustering. Single vacancies and divacancies are allowed to migrate as well as self-interstitial clusters with sizes smaller than 40. We use the values calculated by Adams and Wolfer [42] with molecular dynamics simulations for the binding energy of He with vacancy clusters of different sizes to form He–V complexes. In those calculations values for clusters up to 20 vacancies and 10 He atoms were obtained. We have extrapolated those results to larger number of He atoms in a cluster as well as vacancies.

The migration of helium can occur through different paths. On one hand if He is in an interstitial position it migrates with a low barrier, 0.1 eV, as observed experimentally [43]. When He is in a substitutional site it can migrate through two mechanisms: the dissociative mechanism and the vacancy mechanism. In the case of the dissociative mechanism the substitutional He goes into an interstitial position leaving a vacant site. In the case of the vacancy mechanism a He at a substitutional position can exchange places with a nearby vacancy. The activation energy for this mechanism is often assumed as a first approach to be the one for self-diffusion [44]. In this work we have included both mechanisms for migration: dissociation and vacancy mechanisms. Moreover, since self-interstitials are present in the calculation, another possible mechanism of migration of He is by the interaction of a He substitutional with a self-interstitial resulting in a He interstitial that is very mobile. Values used in this simulation for migration energies of defects are representative of a metal but not quantitative for any specific material. In particular migration energies of self-interstitial clusters of 0.1 eV are considered, higher migration energy for single-vacancy (0.7 eV) and dissociation energy of He substitutional into He interstitial of 1.5 eV.

The nucleation of He–V complexes occurs by migration of He and reaction with isolated vacancies to nucleate higher order He–V clusters. In our calculation all He–V complexes are assumed to be immobile. The nucleation of a void from interaction of a helium atom with pre-existing vacancy clusters, such as those formed during irradiation is very unlikely, as shown by Foreman and Singh [45]. Therefore, in our model large vacancy clusters formed in the cascades cannot transform into voids, and can only contribute to void nucleation through cluster dissolution.

All reactions are considered to be diffusion limited, that is, there is no barrier for reaction between two defects; as soon as two defects are within their capture radius the reaction will occur. The interaction radius between defects is $r = r_{\mathrm{sph}} + \delta$, where δ is the jump distance and r_{sph} is defined as in Eq. (5) above. Since the stress field of self-interstitials is larger than the one of single-vacancies, a larger capture radius is considered for interstitials (r_{I}) interacting with loops (vacancy or interstitial clusters) than for the case of vacancies, r_{v}: $r_{\mathrm{I}} = 1.15 \times r_{\mathrm{v}}$, where r_{v} has been defined above. This therefore includes a bias for the interaction of interstitials with the other defects in the material. We include a sink to both vacancies and interstitials within the simulation box. The capture radius is also biased

with a value of $r_I^s = 1.4 \times r_v^s$, where r_I^s is the capture radius of a self-interstitial to the sink and r_v^s is the capture radius of a vacancy to the sink. This sink mimics the presence of a dislocation, and corresponds to a dislocation density of 2×10^{10} dislocations/cm^2. More details on the model and results can be seen in Ref. [31].

In this paper we show how differences in the source term influences drastically the nucleation and growth of He–V clusters. We use two databases of molecular dynamics simulations of cascades in metals: one for Au obtained at Lawrence Livermore National Laboratory [16] and a second one for Fe obtained by Roger Stoller [15] at Oak Ridge National Laboratory. The energy of the cascades used for these calculations is of 30 keV for Au and 40 keV for Fe. For these two energies selected the average number of defects per cascade is approximately the same in both metals, more precisely 125 pairs of defects for the case of Au and 131 for the case of Fe. Despite the very similar number of defects, the morphology of the damage is quite different as can be seen in the example presented in Fig. 2. In the case of an f.c.c. metal such as Au after the collapse of the cascade produced by the high energy recoil most of the vacancies are forming clusters as shown in Fig. 2(a), where vacancies are the light spheres and self-interstitials are dark. However in the case of a b.c.c. metal such as Fe the vacancies resulting from the cascade collapse are mostly isolated as shown in Fig. 2(b). Self-interstitials form clusters in both Au and Fe cascades although the cluster sizes in the latter are smaller.

Considering exactly the same parameters for migration and dissociation energies of vacancies, self-interstitials and He–V complexes, as well as the same capture radius (or dislocation bias) we have computed the effect of the source term in the nucleation and growth of He–V complexes. This is accomplished by using as the source term the 30 keV Au cascades (that we will call source I) or the 40 keV Fe cascades (source II). For each cascade we include one He atom, or a total of 1000 appm of He per dpa, which corresponds to conditions close to those obtained from helium implantation experiments. A dpa (displacement per atom) is the unit of damage as defined in the ASTM standards [46] and will be used here to describe the irradiation dose. The evolution of vacancies, self-interstitials and He–V complexes has been calculated as a function of dose and temperature. Fig. 3 shows an example of the concentration of He–V clusters as a function of dose

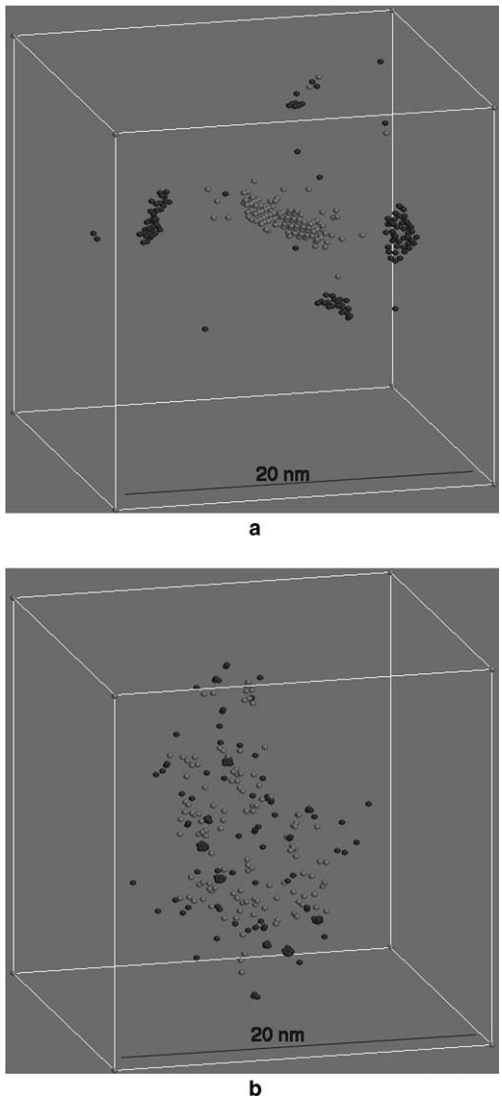

Fig. 2. Cascade damage produced by a 30 keV recoil in Au (a) and by a 40 keV recoil in Fe (b) as obtained from molecular dynamics simulations. The light spheres are vacancies while the dark spheres are interstitials.

and for different temperatures for the case where source I (clustered vacancies) are used. In this particular case a dose rate of 10^{-8} dpa/s was used. At low temperatures the concentration of He–V clusters as a function of dose is independent of temperature, since these He–V clusters are very stable at these temperatures. As the temperature increases He can either dissolve from small He–V clusters and migrate or migrate through the vacancy mechanism joining other clusters and reducing the total cluster density. At even higher temperatures those clusters can dissolve reducing more the total cluster population.

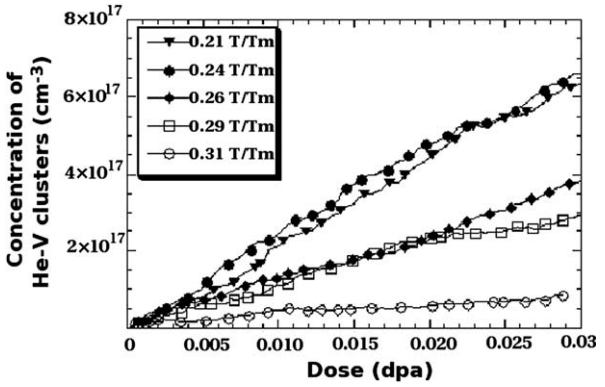

Fig. 3. Concentration of He–V complexes as a function of dose for the case of source I (damage produced in Au), a dose rate of 10^{-8} dpa/s and different temperatures.

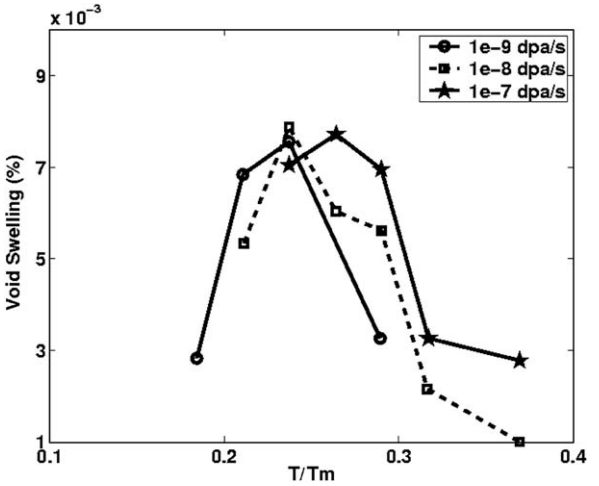

Fig. 4. Void swelling (or change in volume due to vacancies in He–V complexes) as a function of temperature for a total dose of 0.03 dpa and three different dose rates. These results are for the case of source I (damage produced in Au).

However, even more significant than the total population of He–V complexes is the change in volume induced by these defects, or void swelling. Due to the discrete nature of these calculations we can obtain the total number of vacancies in clusters on each type of He–V complexes and extract the total change in volume due to these defects, $\Delta V/V$. This is calculated as

$$\Delta V/V(\phi) = \sum_N C_v^{\mathrm{void}(N)}(\phi) \times \Omega_r(N), \tag{6}$$

where $C_v^{\mathrm{void}(N)}$ is the concentration of vacancies on He–V complexes of size N and $\Omega_r(N)$ is the relaxation volume for a vacancy in a cluster of size N. In this calculation we considered a relaxation volume per vacancy of 0.8Ω, which is the limiting value for voids with more than nine vacancies obtained by Shimomura [47] using molecular dynamics simulations. This change in volume obtained from the kMC calculations is what we will call the void swelling. In this calculation it is considered that those large vacancy clusters formed in the cascade collapse are either forming stacking fault tetrahedra (SFTs) or dislocation loops, therefore due to their collapse into these types of clusters they do not contribute to a change in volume. However, He–V clusters form spherical clusters, avoiding the collapse into these other shapes, and therefore contributing to a change in volume.

Using this approach we have calculated the change in volume as a function of temperature for a particular dose $\phi = 0.03$ dpa and different dose rates for the case of source I. The results of these simulations are shown in Fig. 4. This figure shows how this change in volume is very small at low temperatures and increases as the temperature increases. For the case of 10^{-8} dpa/s the curve has a peak swelling at around $0.24T_m$ for these particular conditions where T_m is the melting point of the material. This dependence of void swelling on temperature is characteristic of f.c.c. metals [48,49], and it is reproduced by the model. The particular position of the swelling peak and the total void swelling values will depend on the material, the dose, the dose rate and the helium per dpa ratio. As an example, copper under fission neutron irradiation with a damage rate of 2×10^{-7} dpa/s and concentration of ~0.3 appm He and ~15 appm H has a swelling peak at around 0.44 T_m [49]. The position of the swelling peak shifts towards lower temperature values as the He concentration increases [49] and as shown in Fig. 4 it also shifts towards lower temperatures with decreasing dose rate. We should point out that the conditions in this simulation are of very high He/dpa ratio and very low dpa rate with results in a swelling peak position at a very low temperature.

We have repeated this set of simulations for the case of source II, where vacancies are mostly isolated and self-interstitial clusters are very small. The calculations were done for a dose rate of 10^{-8} dpa/s and different temperatures. The same value for the relaxation volume of the vacancies in He–V complexes was used. Fig. 5 shows the void swelling curve obtained from the calculation with source I (filled circles) as compared to that obtained

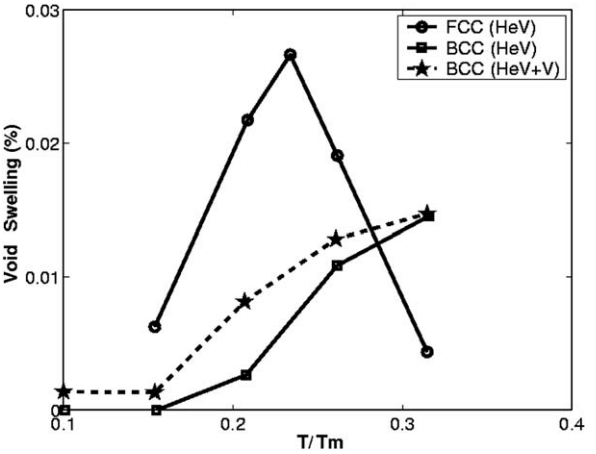

Fig. 5. Void swelling as a function of temperature for the case of source I (circles) and for the case of source II (squares). Dose rate is 10^{-8} dpa/s and total dose is 0.1 dpa.

from source II (filled squares). The dependence with temperature is significantly different.

The reason for this difference is exclusively on the source term, since all other parameters in the model were kept the same. In the case of source I the initial vacancy population is forming clusters. As we mentioned above these clusters cannot contribute to the formation of He–V complexes until they dissolve. Since the concentration of single vacancies is so small the number of He–V clusters and therefore void swelling at very low temperatures is also low. At higher temperatures, when small vacancy clusters can dissolve He–V nuclei are formed and void swelling increases. Only when the temperature is so high that small He–V nuclei are not stable void swelling will decrease.

In the case of source II most of the vacancies are isolated after the cascade collapse. They are, therefore able to form nuclei for He–V complexes. However, the recombination rate between single vacancies and the mobile self-interstitials reduces significantly the vacancy supersaturation. This recombination is much lower in the case of source I due to both the presence of larger self-interstitial clusters and the one-dimensional mobility of these clusters. When the temperature increases such that there is significant mobility of both single vacancies and He, the He–V complexes start to grow and void swelling increases. At temperatures where the stability of small He–V nuclei is short there is a balance between formation and dissolution of these clusters and that could be responsible of the apparent saturation observed for temperatures above 0.3 T_m for this particular example.

Another important result of these simulations is the helium per vacancy ratio obtained on each of the two cases. In the case of source I the number of He atoms per vacancy on each void on average is very small, on the order of 0.3 He per Vacancy. However, in the case of source II, the number of helium per vacancy is larger, around 0.5. The reason for this difference is simple. The total vacancy supersaturation in source II is always smaller than in source I, due to the larger recombination ratio between vacancies and self-interstitials, therefore resulting in lower He–V nuclei. Since the simulations were done for the same total number of helium atoms the He per vacancy ratio must be higher in the case of source II. This is a result of the model that will have to be validated through experiments, such as positron annihilation, although extracting information about the He per vacancy ratio from these experiments is not an easy task.

5. Discussion

Experimental observations reveal that f.c.c. metals behave quite differently with respect to b.c.c. materials in terms of void swelling under irradiation [48]. In general it is observed that b.c.c. materials have high resistance to void swelling while f.c.c. are prone to nucleation and growth of voids. In particular Singh and Evans [48] showed that the temperature dependence of void swelling in these two systems is very different. While f.c.c. metals show a maximum swelling peak, b.c.c. metals have very low swelling rates that remain almost constant at low temperatures and increase gradually after a particular temperature. There is not yet a complete explanation for this difference.

The simulations described above show only the initial stages of the evolution of the damage in the presence of He. The doses reached in these calculations are very small and the sizes of the He–V complexes are only a few nanometers in diameter. Although it is not possible to do a direct comparison between experimental results on void swelling and these simulations there are some similarities that should be pointed out, since these He–V complexes could be the precursors for the formation of experimentally observed bubbles and voids. In particular it is interesting to notice the dependence of the volume changes with temperature obtained from these calculations and those from f.c.c. and

b.c.c. metals. The results of the calculations presented when using clustered vacancies as the initial damage resembles the dependence with temperature observed in metals such as Cu or Ni [48] while when vacancies are isolated after the cascade collapse the curve resembles the dependence observed in metals such as Fe [48]. Since in the case of Fe it has been proved experimentally that some very small spherical clusters can exist without the presence of He [39] we have included in Fig. 5 the contribution to the swelling that could arise from the presence of these small vacancy clusters (open squares in Fig. 5). Even when including these clusters the temperature dependence is not altered.

It is important to notice that in both simulations the dislocation bias considered is the same. The dislocation bias model attributes the differences in swelling between different materials to a difference in the bias. These calculations show that it is possible to have very different evolutions of the HeV cluster populations without a difference in dislocation bias. On the other hand the same assumptions were also included for the case of self-interstitial cluster migration. Therefore it seems it is not necessary to have a population of mobile and immobile self-interstitial clusters in the cascade core to explain differences in void swelling as claimed by the production bias model. It is only the difference in clustering, not only of vacancies, but also of interstitials and the one-dimensional migration of large self-interstitial clusters reaching sinks such as dislocations, grain boundaries or surfaces, that results in different swelling curves.

6. Conclusions

In summary, these simulations show that the morphology of the damage produced during the first few picoseconds in the collapse of a cascade influences significantly the nucleation and growth of defects during irradiation both in pure metals and in the presence of He. For pure metals the number of visible clusters in the case of Cu and Fe is significantly different due to the difference in clustering. In the presence of He the existence of clustered vacancies and the one-dimensional migration of large self-interstitial clusters enhance the formation of He–V clusters due to the high vacancy supersaturation. The presence of a swelling peak is also due to the initial vacancy clustering, since nucleation of voids proceeds through a two step process: dissolution of clusters and stability of small He–V complexes. When most of the vacancies are isolated after cascade collapse and no large clustering of self-interstitials is observed, the vacancy supersaturation decreases due to high recombination ratios, resulting in reduced number of He–V complexes. As a result, for the case of equal He concentration, the He per vacancy ratio will be larger in the second case than in the first one. In view of these results we can conclude that systems with low vacancy and self-interstitial clustering after the cascade collapse will present reduced He–V clustering. The results of these calculations cannot be compared qualitatively to any particular material or experiment and are only intended to show the large influence of the initial cascade damage in the results of a kMC calculation, keeping all other parameters the same.

In order to develop a truly predictive and qualitative kMC model for metals such as Fe or Cu in the presence of He many fundamental studies must be done as pointed out in Ref. [50]. In particular, a better understanding of the mechanisms for He mobility in different metals must be achieved, as well as the type of mechanism that dominates for different conditions of dose, dose rate, He per dpa ratio and temperature. Such an understanding can only be achieved through tailored experiments and kMC calculations. In the particular case of Fe the interaction of self-interstitials and vacancies with the impurities present in this metal such as carbon must also be understood.

Although kMC is an efficient algorithm for defect evolution, reaching high concentrations, in particular when one-dimensional diffusion occurs can be computationally expensive. A similar approach to the kMC model explained here is the so called Event Kinetic Monte Carlo [34]. This model has some approximations but can be more efficient than the OKMC for certain cases, in particular for low defect densities. For high densities however it might be necessary to make use of continuum models in order to reach doses of several dpa.

Acknowledgements

We would like to thank Roger Stoller for providing his cascades in Fe and Meijie Tang and Eduardo Alonso for the cascades in Au. This work was carried out under the auspices of the US Department of Energy by Lawrence Livermore National Laboratory under contract W-7405-Eng-48. One of the authors (MJC) wants to thank the Spanish MEC for support under the Ramon y Cajal program. This

work was partly supported by the PERFECT European Integrated Project under Contract No. FI6O-CT-508840.

References

[1] D.G. Besco, Computer Simulation of Point Defect Annealing in Metals, USA-AEC Report GEMP-644, October 1967.
[2] D.G. Doran, Radiat. Eff. 2 (1970) 249.
[3] D.G. Doran, R.A. Burnett, in: P.C. Gehlen, J.K.R. Beeler, R.I. Jafee (Eds.), Interatomic Potentials and Simulations of Lattice Defects, Plenum, New York, NY, 1972, p. 403.
[4] H.L. Heinisch, Radiat. Eff. Def. Solids 113 (1990) 53.
[5] B.D. Wirth, J. Nucl. Mater., these Proceedings.
[6] C. Domain, C.S. Becquart, L. Malerba, J. Nucl. Mater. 335 (2004) 121.
[7] M.J. Caturla, N. Soneda, E. Alonso, B.D. Wirth, T. Diaz de la Rubia, J.M. Perlado, J. Nucl. Mater. 276 (2000) 13.
[8] N. Soneda, T. Diaz de la Rubia, Philos. Mag. A 78 (1998) 995.
[9] N. Soneda, S. Ishino, A. Takahashi, K. Dohi, J. Nucl. Mater. 323 (2003) 169.
[10] L. Pelaz, M. Jaraiz, G.H. Gilmer, H.J. Gossmann, C.S. Rafferty, D.J. Eaglesham, J.M. Poate, Appl. Phys. Lett. 70 (1997) 2285.
[11] M. Johnson, M.J. Caturla, T. Diaz de la Rubia, J. Appl. Phys. 84 (1998) 1963.
[12] D.J. Bacon, T. Diaz de la Rubia, J. Nucl. Mater. 216 (1994) 275.
[13] Yu.N. Osetsky, D.J. Bacon, Nucl. Instrum. Meth. B 180 (2001) 85.
[14] K. Nordlund, F. Gao, Appl. Phys. Lett. 74 (1999) 2720.
[15] R.E. Stoller, G.R. Odette, B.D. Wirth, J. Nucl. Mater. 251 (1997) 49.
[16] E. Alonso, M.J. Caturla, M. Tang, H. Huang, T. Diaz de la Rubia, Mater. Res. Soc. 731 (1997) 367.
[17] M.J. Caturla, M. Wall, E. Alonso, T. Diaz de la Rubia, T. Felter, M. Fluss, J. Nucl. Mater. 276 (2000) 186.
[18] T. Diaz de la Rubia, W.J. Phythian, J. Nucl. Mater. 191–194 (1992) 108.
[19] M.J. Caturla, T. Diaz de la Rubia, M. Victoria, K. Corzine, M. James, G.A. Greene, J. Nucl. Mater. 296 (2001) 90.
[20] Yu.N. Osetsky, A. Serra, B.N. Singh, S.I. Golubov, Philos. Mag. A 80 (2000) 2131.
[21] B.D. Wirth, G.R. Odette, D. Maroudas, G.E. Lucas, J. Nucl. Mater. 244 (1997) 185.
[22] N. Soneda, T. Diaz de la Rubia, Philos. Mag. A 81 (2001) 331.
[23] C. Domain, C.S. Becquart, Phys. Rev. B 65 (2002) 024103.
[24] Chu Chun Fu, F. Willaime, Phys. Rev. Lett. 92 (2004) 175503.
[25] J. Marian, B.D. Wirth, A. Caro, B. Sadigh, G.R. Odette, J.M. Perlado, T. Diaz de la Rubia, Phys. Rev. B 65 (2002) 144102.
[26] L.K. Mansur, J. Nucl. Mater. 216 (1994) 97.
[27] W.G. Wolfer, F.A. Garner, Radiat. Eff. 78 (1983) 275.
[28] G.W. Greenwood, A.J.E. Foreman, D.E. Rimmer, J. Nucl. Mater. 4 (1959) 305.
[29] B.N. Singh, S.J. Zinkle, J. Nucl. Mater. 206 (1993) 212.
[30] C.H. Woo, B.N. Singh, Philos. Mag. A 65 (1992) 889.
[31] M.J. Caturla, T. Diaz de la Rubia, M. Fluss, J. Nucl. Mater. 323 (2003) 163.
[32] J.F. Ziegler, J.P. Biersack, U. Littmark, in: J.F. Ziegler (Ed.), The Stopping and Range of Ions in Solids, vol. 1, Pergamon, New York, 1985.
[33] M.T. Robinson, Phys. Rev. B 40 (1989) 10717.
[34] Chu-Chun Fu, J. Dalla-Torre, F. Willaime, J.-L. Bocquet, A. Barbu, Nature Mater. 4 (2005) 68.
[35] T. Hudson, S.L. Dudarev, M.J. Caturla, A.P. Sutton, Philos. Mag. 85 (2005) 661.
[36] L.Z. Sun, N.M. Ghoniem, S.H. Tong, B.N. Singh, J. Nucl. Mater. 283–287 (2000) 741.
[37] Y. Dai, M. Victoria, Mater. Res. Soc. Symp. Proc. 439 (1997) 319.
[38] B.L. Eyre, A.F. Bartlett, Philos. Mag. 12 (1965) 261.
[39] M. Eldrup, B.N. Singh, J. Nucl. Mater. 276 (2000) 269.
[40] C. Domain, C.S. Becquart, J. Foct, Phys. Rev. B 69 (2004) 144112.
[41] J. Marian, B.D. Wirth, J.M. Perlado, Phys. Rev. Lett. 88 (2002) 255507.
[42] J.B. Adams, W.G. Wolfer, J. Nucl. Mater. 166 (1989) 235.
[43] H. Ullmaier, Landolt-Bornstein, Numerical Data and Functional Relationships in Science and Technology, New Series, vol. III/25, 1991, p. 381.
[44] V. Sciani, P. Jung, Radiat. Eff. 78 (1983) 87.
[45] A.J.E. Foreman, B.N. Singh, Radiat. Eff. Def. Solids 113 (1990) 175.
[46] M.J. Norgett, M.T. Robinson, I.M. Torrens, Nucl. Eng. Des. 33 (1975) 50.
[47] Y. Shimomura, Mater. Chem. Phys. 50 (1997) 139.
[48] B.N. Singh, J.H. Evans, J. Nucl. Mater. 226 (1995) 277.
[49] S.J. Zinkle, K. Farrell, J. Nucl. Mater. 168 (1989) 262.
[50] H. Trinkaus, B.N. Singh, J. Nucl. Mater. 323 (2003) 229.